

1 **A total energy error analysis of dynamical cores and**
2 **physics-dynamics coupling in the Community Atmosphere**
3 **Model (CAM)**

4 **Peter H. Lauritzen^{1*}, and David L. Williamson¹**

5 ¹National Center for Atmospheric Research, Boulder, Colorado, USA

6 **Key Points:**

- 7 • Spurious total energy dissipation in dynamical core is $-0.3W/m^2$ to $-1W/m^2$ at 1
8 degree
9 • Constant-pressure assumption in physics leads to $0.3W/m^2$ spurious total energy
10 source
11 • There can easily be compensating errors in total energy budget

*1850 Table Mesa Drive, Boulder, Colorado, USA

Corresponding author: Peter Hjort Lauritzen, pel@ucar.edu

12 **Abstract**

13 A closed total energy (TE) budget is of utmost importance in coupled climate system
 14 modeling; in particular, the dynamical core or physics-dynamics coupling should ideally
 15 not lead to spurious TE sources/sinks. To assess this in a global climate model, a detailed
 16 analysis of the spurious sources/sinks of TE in NCAR's Community Atmosphere Model
 17 (CAM) is given. This includes spurious sources/sinks associated with the parameteriza-
 18 tion suite, the dynamical core, TE definition discrepancies and physics-dynamics coupling.
 19 The latter leads to a detailed discussion of the pros and cons of various physics-dynamics
 20 coupling methods commonly used in climate/weather modeling.

21 **1 Introduction**

22 In coupled climate modeling with prognostic atmosphere, ocean, land, land-ice, and
 23 sea-ice components, it is important to conserve total energy (TE) to a high degree in each
 24 component individually and in the complete model to avoid spurious long term trends in
 25 the simulated Earth system. Conservation of TE in this context refers to having a closed
 26 TE budget. For example, the TE change in a column in the atmosphere is exactly balanced
 27 by the net sources/sinks given by the fluxes through the column. The fluxes into the at-
 28 mospheric component from the surface models must be balanced by the fluxes in the re-
 29 spective surface components and so on. Henceforth we will focus only on the atmospheric
 30 component which, in a numerical model, is split into a resolved-scale component (the dy-
 31 namical core) and a sub-grid-scale component (parameterizations or, in modeling jargon,
 32 physics). While there have been many studies on energy flow in the Earth system through
 33 analysis of re-analysis data and observations [Trenberth and Fasullo, 2018, and references
 34 herein], there has been less focus on spurious TE sources/sinks in numerical models.

35 The atmospheric equations of motion conserve TE but the discretizations used in cli-
 36 mate and weather models are usually not inherently TE conservative. Exact conservation
 37 is probably not necessary but conservation to within $\sim 0.01 \text{ W/m}^2$ has been considered
 38 sufficient to avoid spurious trends in century long simulations [Boville, 2000; Williamson
 39 *et al.*, 2015]. Spurious sources and sinks of TE can be introduced by the dynamical core,
 40 physics, physics-dynamics coupling as well as discrepancies between the TE of the con-
 41 tinuous and discrete equations of motion and for the physics. Hence the study of TE con-
 42 servation in comprehensive models of the atmosphere quickly becomes a quite complex
 43 and detailed matter. In addition there can easily be compensating errors in the system as a
 44 whole.

45 Here we focus on versions of the Community Atmosphere Model (CAM) that use
 46 the spectral-element [SE, Lauritzen *et al.*, 2018] and finite-volume [FV, Lin, 2004] dy-
 47 namical cores. These dynamical cores couple with physics in a time-split manner, i.e.
 48 physics receives a state updated by dynamics [see Williamson, 2002, for a discussion
 49 of time-split versus process split physics-dynamics coupling in the context of CAM]. In
 50 its pure time-split form the physics tendencies are added to the state previously produced
 51 by the dynamical core and the resulting state provides the initial state for the subsequent
 52 dynamical core calculation. We refer to this as *state-updating* (`ftype=1` in CAM code).
 53 Alternatively, when the dynamical core adopts a shorter time step than the physics, say
 54 `nsplit` sub-steps, then $(1/\text{nsplit})$ th of the physics-calculated tendency is added to the
 55 state before each dynamics sub-step. We refer to this modification of time-splitting as
 56 *dribbling* (`ftype=0`). CAM-FV uses the *state-update* (`ftype=1`) approach while CAM-SE
 57 has options to use *state-update* (`ftype=1`), *dribbling* (`ftype=0`) or a combination of the
 58 two i.e. mass-variables use *state-updating* and remaining variables use *dribbling*. We refer
 59 to this as *combination* (`ftype=2`). The *dribbling* variants can lead to spurious sources or
 60 sinks of TE (and mass) referred to here as physics-dynamics coupling errors.

61 The dynamical core usually has inherent or specified filters to control spurious noise
 62 near the grid scale which will lead to energy dissipation [Thuburn, 2008; Jablonowski

and Williamson, 2011]. Similarly models often have sponge layers to control the solution near the top of the model that may be a sink of TE. There are examples of numerical discretizations of the adiabatic frictionless equations motion that are designed so that TE is conserved in the absence of time-truncation and filtering errors [e.g., Eldred and Randall, 2017; McRae and Cotter, 2013], e.g., mimetic spectral-element discretizations such as the one used in the horizontal in CAM-SE [Taylor, 2011]. These provide consistency between the discrete momentum and thermodynamic equations leading to global conservation associated with the conversion of potential to kinetic energy. In spectral transform models it is customary to add the energy change due to explicit diffusion on momentum back as heating (referred to as frictional heating), so that the diffusion of momentum does not affect the TE budget [see, e.g., p.71 in Neale et al., 2012]. This is also done in CAM-SE [Lauritzen et al., 2018].

The purpose of this paper is to provide a detailed global TE analysis of CAM. We assess TE errors due to various steps in the model algorithms. The paper is outlined as follows. In section 2 the continuous TE formulas are given and a detailed description of spurious TE sources/sinks that can occur in a model as a whole, and the associated diagnostics used to perform the TE analysis, are defined. In section 3 the model is run in various configurations to assess their effects on TE conservation. This includes various physics-dynamics coupling experiments leading to a rather detailed discussion of mass budget closure. We also investigate the effect of using a limiter in the vertical remapping of momentum, assess energy discrepancy errors and impacts on TE of simplifying surface conditions and dry atmosphere experiments. The paper ends with conclusions.

2 Method

2.1 Defining total energy (TE)

In the following it is assumed that the model top and bottom are coordinate surfaces and that there is no flux of mass through the model top and bottom. In a dry hydrostatic atmosphere the TE equation integrated over the entire sphere is given by

$$\frac{d}{dt} \int_{z=z_s}^{z=z_{top}} \iint_S E_v \rho^{(d)} dA dz = \int_{z=z_s}^{z=z_{top}} \iint_S F_{net} \rho^{(d)} dA dz, \quad (1)$$

[e.g., Kasahara, 1974] where F_{net} is net flux calculated by the parameterizations (e.g., heating and momentum forcing), d/dt the total/material derivative, z_s is the height of the surface, S the sphere, $\rho^{(d)}$ the density of dry air, E_v is the TE and dA is an infinitesimal area on the sphere. E_v can be split into kinetic energy $K = \frac{1}{2}\mathbf{v}^2$ (\mathbf{v} is the wind vector), internal energy $c_v^{(d)}T$, where $c_v^{(d)}$ is the heat capacity of dry air at constant volume, and potential energy $\Phi = gz$

$$E_v = K + c_v^{(d)}T + \Phi. \quad (2)$$

If the vertical integral is performed in a mass-based vertical coordinate, e.g., pressure, then the integrated TE equation for a dry atmosphere can be written as

$$\frac{d}{dt} \int_{p=p_s}^{p=p_{top}} \iint_S E_p dA dp + \frac{d}{dt} \iint_S \Phi_s p_s dA = \int_{p=p_s}^{p=p_{top}} \iint_S F_{net} dA dp, \quad (3)$$

[e.g., Kasahara, 1974] where

$$E_p = K + c_p^{(d)}T. \quad (4)$$

In a moist atmosphere, however, there are several definitions of TE used in the literature related to what heat capacity is used for water vapor and whether or not condensates are accounted for in the energy equation. To explain the details of that we focus on the energy equation for CAM-SE.

CAM-SE is formulated using a terrain-following hybrid-sigma vertical coordinate η but the coordinate levels are defined in terms of dry air mass per unit area ($M^{(d)}$) instead of total air mass; $\eta^{(d)}$ [see Lauritzen et al., 2018, for details]. In such a coordinate

106 system it is convenient to define the tracer state in terms of a dry mixing ratio instead of
 107 moist mixing ratio

$$m^{(\ell)} \equiv \frac{\rho^{(\ell)}}{\rho^{(d)}}, \text{ where } \ell = 'wv', 'cl', 'ci', 'rn', 'sw', \quad (5)$$

108 where $\rho^{(d)}$ is the mass of dry air per unit volume of moist air and $\rho^{(\ell)}$ is the mass of the
 109 water substance of type ℓ per unit volume of moist air. Moist air refers to air containing
 110 dry air ('d'), water vapor ('wv'), cloud liquid ('cl'), cloud ice ('ci'), rain amount ('rn')
 111 and snow amount ('sw'). For notational purposes define the set of all components of air

$$\mathcal{L}_{all} = \{'d', 'wv', 'cl', 'ci', 'rn', 'sw'\}, \quad (6)$$

112 Define associated heat capacities at constant pressure $c_p^{(\ell)}$. We refer to condensates as being
 113 *thermodynamically and inertially active* if they are included in the thermodynamic
 114 equation and momentum equations. E.g. if the thermodynamic equation is formulated
 115 in terms of temperature the energy conversion term includes a generalized heat capacity
 116 which is a function of the condensates and their associated heat capacities [see, e.g., sec-
 117 tion 2.3 in *Lauritzen et al., 2018*]. Similarly the weight of the condensates is included in
 118 the pressure field and pressure gradient force. How many and which condensates are ther-
 119 modynamically/inertially active in the dynamical core is controlled with namelist `qsize_condensate_loading`.
 120 If `qsize_condensate_loading=1` only water vapor ('wv') is active, `qsize_condensate_loading=3`
 121 'wv', 'cl', and 'ci' are active, and if `qsize_condensate_loading=5` then 'wv', 'cl', 'ci', 'rn',
 122 and 'sw' are included.

123 Using the $\eta^{(d)}$ vertical coordinate and dry mixing ratios the TE (per unit area) that
 124 the frictionless adiabatic equations of motion in the CAM-SE dynamical core conserves is

$$\widehat{E}_{dyn} = \frac{1}{\Delta S} \int_{\eta=0}^{\eta=1} \iint_S \left(\frac{1}{g} \frac{\partial M^{(d)}}{\partial \eta^{(d)}} \right) \sum_{\ell \in \mathcal{L}_{all}} \left[m^{(\ell)} \left(K + c_p^{(\ell)} T + \Phi_s \right) \right] dA d\eta^{(d)}, \quad (7)$$

125 where ΔS is the surface area of the sphere, Φ_s is the surface geopotential and (\cdot) refers to
 126 the global average.

127 In the CAM physical parameterizations a different definition of TE is used. Due to
 128 the evolutionary nature of the model development, the parameterizations have not yet been
 129 converted to match the SE dynamical core. For the computation of TE, condensates are
 130 assumed to be zero and the heat capacity of moisture is the same as for dry air. This is
 131 equivalent to using a moist mass (dry air plus water vapor) but c_p of dry air:

$$\widehat{E}_{phys} = \frac{1}{\Delta S} \int_{\eta=0}^{\eta=1} \iint_S \left(\frac{1}{g} \frac{\partial M^{(d)}}{\partial \eta^{(d)}} \right) \left(1 + m^{(wv)} \right) \left[\left(K + c_p^{(d)} T + \Phi_s \right) \right] dA d\eta^{(d)}. \quad (8)$$

132 We note that earlier versions of CAM using the spectral transform dynamical core used
 133 c_p of moist air. The adiabatic, frictionless equations of motion in the CAM-SE dynamical
 134 core can be made consistent with E_{phys} by not including condensates in the mass/pressure
 135 field as well as energy conversion term in the thermodynamic equation and setting the
 136 heat capacity for moisture to $c_p^{(d)}$ [Taylor, 2011]. We refer to this version of CAM-SE col-
 137 orredcombined with *state-updating* (`ftype=1` physics-dynamics coupling as the *energy*
 138 *consistent* version ; i.e. the same continuous formula for energy is used in both dynamics
 139 and physics, and there are no physics-dynamics coupling errors.

140 2.2 Some remarks on local energy conservation

141 Although this paper focuses on global TE errors, it is important to note that en-
 142 ergy errors occur locally. For example, whenever an air parcel containing water undergoes
 143 a phase change (in the parameterizations) its temperature and enthalpy (energy) should
 144 change but its mass should not. When the air parcel gains or loses water via sedimenta-
 145 tion or precipitation (or via a fixer or borrower to maintain some physical property like

positive definiteness), then it has implications for the mass and heat content, and heat capacity of the parcel. In turn, that affects the energy and mass of the column and thereby affects the global TE budget. So anything that changes these state variables locally has implications for the TE budget.

An example of an inconsistency in CAM physics is that surface pressure is held fixed during physical parameterization updates but water vapor, and hence surface pressure, does change during sedimentation/precipitation and an inconsistency appears in the mass and energy budget (see item 2 in Section 2.3). Similarly, if a ‘clipper’ is used on water vapor or condensates to avoid (unphysical) negative mixing ratios (more details in section 3.2) and this is not accounted for in the thermodynamics or through a surface flux, that ‘clipping’ will produce an energy source. In the dynamical core TE is not conserved locally in each column as there is a horizontal flux of energy between columns; but the local energy budget should, ideally, be closed and thereby globally TE should be conserved. If a dynamical core does not inherently conserve dry air mass and/or water mass then a spurious source of TE is inevitable (unless fixers are applied).

2.3 Spurious energy sources and sinks

In a weather/climate model TE conservation errors can appear in many places throughout the algorithm. Below is a general list of where conservation errors can appear with specific examples from CAM:

1. *Parameterization errors*: Individual parameterizations may not have a closed energy budget ; for example, they may not have been designed to conserve TE or they may conserve a different TE. CAM parameterizations are required to have a closed energy budget under the assumption that pressure remains constant during the computation of the subgrid-scale parameterization tendencies. In other words, the TE change in the column is exactly balanced by the net sources/sinks given by the fluxes through the column.
2. *Pressure work error*: That said, if parameterizations update specific humidity then the surface pressure changes (e.g., moisture entering or leaving the column). In that case the pressure changes which, in turn, changes TE. This is referred to as *pressure work error* [section 3.1.8 in Neale et al., 2012].
3. *Continuous TE formula discrepancy*: If the continuous equations of motion for the dynamical core conserve a TE different from the one used in the parameterizations then an energy inconsistency is present in the system as a whole. This is the case with the new version of CAM-SE that conserves a TE that is more accurate and comprehensive than that used in the CAM physics package as discussed above. As also noted above, this mismatch arose from the evolutionary nature of the model development and not by deliberate design; and should be eliminated in the future.
4. *Dynamical core errors*: Energy conservation errors in the dynamical core, not related to physics-dynamics coupling errors, can arise in multiple parts of the algorithms used to solve the equations of motion. For dynamical cores employing filtering [e.g., limiters in flux operators Lin, 2004] and/or possessing inherent damping which controls small scales, it is hard to isolate their energy dissipation from other errors in the discretization. If a hyperviscosity term or some other diffusion is added to the momentum equation, then one can diagnose the local energy dissipation from such damping and add a corresponding heating to balance it (frictional heating). There may also be energy loss from viscosity applied to other variables such as temperature or pressure which is harder to compensate. Here is a break-down relevant to CAM-SE using a floating Lagrangian vertical coordinate:
 - Horizontal inviscid dynamics: Energy errors resulting from solving the inviscid, adiabatic equations of motion.
 - Hyperviscosity: Filtering errors.

- 197 • Vertical remapping: The vertical remapping algorithm from Lagrangian to Euler-
 198 ian reference surfaces does not conserve TE.
 199 • Near round-off negative values of water vapor which are filled to a minimal
 200 value without compensation.

201 If a dynamical core is not inherently mass-conservative with respect to dry air, wa-
 202 ter vapor and condensates then TE conservation is affected since

$$\int_{\eta=0}^{\eta=1} \iint_S \left(\frac{1}{g} \frac{\partial M^{(d)}}{\partial \eta^{(d)}} \right) \sum_{\ell \in \mathcal{L}_{all}} [m^{(\ell)}] dA d\eta^{(d)} \quad (9)$$

203 is not conserved. Henceforth we assume that the dynamical core is based on an
 204 inherently mass-conservative formulation which is the case for CAM-SE and CAM-
 205 FV.

206 5. *Physics-dynamics coupling (PDC)*: Assume that physics computes a tendency. Usu-
 207 ally the tendency (forcing) is passed to the dynamical core which is responsible for
 208 adding the tendencies to the state. PDC energy errors can be split into three types:

- 209 • ‘Dribbling’ errors (or, equivalently, temporal PDC errors): If the TE increment
 210 from the parameterizations does not match the change in TE when the tenden-
 211 cies are added to the state in the dynamical core, then there will be a spurious
 212 PDC error. This will not happen with the *state-update* approach in which the
 213 tendencies are added immediately after physics and before the dynamical core
 214 advances the solution in time. The PDC ‘dribbling’ errors can be split into 3 con-
 215 tributions.:

216 *Thermal energy ‘dribbling’ error*: PDC errors in temperature tendencies occur
 217 because the T -increment (call it ΔT) that the parameterizations prescribe leads
 218 to a dry thermal energy change of $\Delta M^{(d)} \Delta T$ which will not match the equivalent
 219 dry thermal energy change when the temperature tendency is added in smaller
 220 chunks in the dynamical core during the ‘dribbling’ of ΔT . The discrepancy
 221 occurs because $\Delta M^{(d)}$ changes during each dynamics time-step and hence the
 222 thermal energy change due to physics forcing accumulated during the ‘dribbling’
 223 will not equal $\Delta M^{(d)} \Delta T$. This error could possibly be eliminated by using ther-
 224 mal energy forcing instead of temperature increments.

225 *Kinetic energy ‘dribbling’ error*: Similarly, PDC errors in velocity component
 226 forcing increments ($\Delta u, \Delta v$) occur because the dry kinetic energy change of $\Delta M^{(d)} [(\Delta u)^2 + (\Delta v)^2]$
 227 will not match the equivalent dry kinetic energy change when ‘dribbling’ veloc-
 228 ity component forcing increments ($\Delta u, \Delta v$). It is less clear how to eliminate this
 229 error as kinetic energy is a quadratic quantity.

230 *Mass ‘clipping’ (affects all TE terms)*: A similar PDC error for mass-variables
 231 such as vapor vapor forcing, cloud liquid, etc. can occur when the mass-tendencies
 232 are ‘dribbled’ during the dynamical core integration. The dynamical core trans-
 233 port of mass variables will move mass around in the horizontal and vertical while
 234 the ‘dribbled’ physics mass increments are applied in the same location; in that
 235 situation a negative mass-increment from the parameterizations may be larger
 236 than the mass available to remove. This can lead to a spurious source mass if
 237 there is logic in the dynamical core preventing mixing ratios/mass to become
 238 negative. This is referred to as ‘clipping’ PDC errors and precess is described/discussed
 239 in detail in Section 3.2.1. The ‘clipping’ change the water mass budget without
 240 accounting for it in water fluxes or in the thermodynamics and hence lead to a
 241 TE conservation errors (both kinetic and thermal energy).

- 242 • *Change of vertical grid/coordinate errors*: If the vertical coordinates in physics
 243 and in the dynamical core are different then there can be spurious PDC energy
 244 errors even when using the state-update method for adding tendencies to the dy-
 245 namical core state. For example, many non-hydrostatic dynamical cores [e.g.
 246 Skamarock et al., 2012] use a terrain-following height coordinate whereas physics
 247 uses pressure.

- 248 • *Change of horizontal grid errors:* If the physics tendencies are computed on a
 249 different horizontal grid than the dynamical core then there can be spurious en-
 250 ergy errors from mapping tendencies and/or variables between horizontal grids
 251 [e.g., *Herrington et al.*, 2018].
- 252 6. *Compensating Energy fixers:* To avoid TE conservation errors which could accu-
 253 mulate and ultimately lead to a climate drift, it is customary to apply an arbitrary
 254 energy fixer to restore TE conservation. Since the spatial distribution of many en-
 255 ergy errors, in general, is not known, global fixers are used. In CAM a uniform in-
 256 crement is added to the temperature field to compensate for TE imbalance from all
 257 processes, i.e. dynamical core, physics-dynamics coupling, TE formula discrepancy,
 258 energy change due to pressure work **error**, and possibly parameterization errors if
 259 present.

260 **2.4 Diagnostics**

261 The discrete global averages ($\widehat{\cdot}$) are computed consistent with the discrete model grid
 262 as outlined in section 2.2. of *Lauritzen et al.* [2014]. The TE global average tendency is
 263 denoted

$$\partial \widehat{E} \equiv \frac{d\widehat{E}}{dt}. \quad (10)$$

264 By computing the global TE averages \widehat{E} at appropriate places in the model algorithms,
 265 we can directly compute $\partial \widehat{E}$ due to various processes (such as viscosity, vertical remap-
 266 ping, physics-dynamics coupling, pressure work **error**, etc.) by differencing \widehat{E} from after
 267 and before the algorithm takes place. This has been implemented using CAM history in-
 268 frastructure by computing column integrals of energy at various places in CAM and out-
 269 putting the 2D energy fields. CAM history internally handles accumulation and averag-
 270 ing in time at each horizontal grid point. The global averages are computed externally
 271 from the grid point vertical integrals on the history files (stored in double precision). The
 272 places in CAM where we compute/capture the grid point vertical integral E are named us-
 273 ing three letters where the first letter refers to whether the vertical integral is performed
 274 in physics ('p') or in the dynamical core ('d'). The trailing two letters refer to the specific
 275 location in dynamics or physics. For example, 'BP' refers to 'Before Physics' and 'AP'
 276 to 'After Physics'; the associated total energies are denoted E_{pBP} and E_{pAP} , respectively.
 277 The TE tendency from the parameterizations is the difference between E_{pBP} and E_{pAP}
 278 divided by the time-step. The terms and tendencies are then averaged globally externally
 279 to the model. The pseudo-code in Figure 1 defines the acronyms in terms of where in the
 280 CAM-SE algorithm the TE vertical integrals are computed and output. For details on the
 281 CAM-SE algorithm please see *Lauritzen et al.* [2018].

282 Before defining the individual terms in detail we briefly review the model time step-
 283 ping sequence starting with the physics component as illustrated in Figure 1. The energy
 284 fixer is applied first to compensate for the spurious net energy change from all compo-
 285 nents introduced during the previous time step. We will describe this in more detail af-
 286 ter the various sources and sinks are elucidated. The parameterizations are applied next
 287 and are required to be energy conserving. They update the state and accumulate the total
 288 physics tendency (forcing). At this stage the state is saved for use in the energy fixer in
 289 the next time step. Any changes in the global average energy after this are spurious and
 290 are compensated by the fixer. The parameterizations update the water vapor but not the
 291 moist pressure, implying a non-physical change in the dry mass of the atmosphere. The
 292 dry mass correction corrects the dry mass back to its proper value.

293 The forcing (physics tendency) from the parameterizations is passed to the dynam-
 294 ical core. If the physics and dynamics operate on different grids, the forcing is remapped
 295 here. The dynamics operates on a shorter time step **than** the physics and is sub-stepped.
 296 The remapped **physics increment** is applied to the dynamics state, saved from the end of
 297 the previous dynamics step, using either *state-updating*, *dribbling*, or *combination* as de-

scribed in the introduction. The dynamics then advances the adiabatic frictionless flow in the floating Lagrangian layers over a further set of sub-steps. Hyperviscosity is applied next with further sub-stepping required for computational stability of the explicit discrete approximations. The energy loss from the specified momentum viscosity is **calculated** locally and is balanced by adding a local change to the temperature, referred to as *frictional heating*. This set of dynamics sub-steps is followed by the vertical remapping from Lagrangian to Eulerian reference layers. The remapping is required to provide layers consistent with the parameterization formulations. The vertical remapping sub-steps are required for stability if the Lagrangian layers become too thin.

At the end of the dynamics, the state is saved to be used by the dynamics the next time step and is also passed to the physics, with a remapping if the dynamics and physics grids differ. At the beginning of the physics the difference in energy between this state and the state saved after the physics during the previous time step is the amount needed to be added or subtracted by the energy fixer. It represents the accumulation of all spurious sources from the dry mass correction, remappings between physics and dynamics grids (if applicable), dynamical core, differing energy definitions (if present), hyerviscosity, and vertical remapping.

We now define the following energy tendencies corresponding to the itemized list in section 2.3 with references to terms indicated in Figure 1. We start just after the energy fixer which will be defined at the end.

1. $\partial\widehat{E}^{(param)}$: TE tendency due to parameterizations. In CAM the TE budget for each parameterization is closed (assuming pressure is unchanged) so $\partial\widehat{E}^{(param)}$ is balanced by net fluxes in/out of the physics columns. Note that this is the only energy tendency that is not spurious since CAM parameterizations have a closed TE budget. This TE tendency is discretely computed as

$$\partial\widehat{E}_{phys}^{(param)} = \frac{\widehat{E}_{pAP} - \widehat{E}_{pBP}}{\Delta t_{phys}}, \quad (11)$$

where Δt_{phys} is the physics time-step (default 1800s) and the subscript *phys* on $\partial\widehat{E}$ refers to the energy tendency computed in CAM physics.

2. $\partial\widehat{E}^{(pwork)}$: Total spurious energy tendency due to pressure work **error**

$$\partial\widehat{E}_{phys}^{(pwork)} = \frac{\widehat{E}_{pAM} - \widehat{E}_{pAP}}{\Delta t_{phys}}. \quad (12)$$

Since CAM-SE dynamical core is based on a dry-mass vertical coordinate the pressure work **error** takes place implicitly in the dynamical core. But the TE tendency due to pressure work **error** is conveniently computed in physics since dynamical cores based on a moist vertical coordinate (e.g., CAM-FV) require pressure and moist mixing ratios to be adjusted for dry mass conservation and tracer mass conservation [section 3.1.8 in *Neale et al.*, 2012]. The difference of TE after and before this adjustment is the TE tendency due to pressure work **error**. In a dry mass vertical coordinate based on dry mixing ratios neither dry mass layer thickness nor dry mixing ratios need to be adjusted to take into account moisture changes in the column. For labeling purposes, the 'total forcing' associated with physics (at least in CAM) consists of parameterizations, pressure work **error** and TE fixer, although strictly speaking the fixer includes components from the dynamics as will be seen.

$$\partial\widehat{E}_{phys}^{(phys)} = \partial\widehat{E}_{phys}^{(param)} + \partial\widehat{E}_{phys}^{(pwork)} + \partial\widehat{E}_{phys}^{(efix)} = \frac{\widehat{E}_{pAM} - \widehat{E}_{pBF}}{\Delta t_{phys}}. \quad (13)$$

where the energy fixer TE tendency is

$$\partial\widehat{E}_{phys}^{(efix)} = \frac{\widehat{E}_{pBP} - \widehat{E}_{pBF}}{\Delta t_{phys}}. \quad (14)$$

- 347 After all the TE budget terms have been defined, the exact composition of $\partial\widehat{E}_{phys}^{(efix)}$
 348 will be presented.
- 349 3. $\partial\widehat{E}^{(discr)}$: If the physics uses a TE definition different from the TE that the
 350 continuous equations of motion in the dynamical core conserve (i.e. in the absence of
 351 discretization errors), then there is a TE discrepancy tendency. This complicates
 352 the energy analysis as one can not compare TE computed in physics \widehat{E}_{phys} directly
 353 with TE computed in the dynamical core \widehat{E}_{dyn} . This makes errors associated with
 354 this discrepancy tricky to assess. That said, the TE tendencies computed using the
 355 dynamical core TE formula $\partial\widehat{E}_{dyn}$ are well defined (self consistent) and similarly
 356 for TE tendencies computed using the ‘physics formula’ for TE, $\partial\widehat{E}_{phys}$.
- 357 4. The TE tendency from the dynamical core is split into several terms: Horizontal
 358 adiabatic dynamics (dynamics excluding physics forcing tendency)

$$\partial\widehat{E}_{dyn}^{(2D)} = \frac{\widehat{E}_{dAD} - \widehat{E}_{dBd}}{\Delta t_{dyn}}, \quad (15)$$

359 where over a single dynamics sub-step $\Delta t_{dyn} = \frac{\Delta t_{phys}}{n_{split} \times r_{split}}$ (the loop bounds
 360 n_{split} , r_{split} , etc. are explained in Figure 1).

361 In CAM-SE the viscosity is explicit so one can compute the TE tendency due to
 362 hyperviscosity and its associated frictional heating

$$\partial\widehat{E}_{dyn}^{(hvvis)} = \frac{\widehat{E}_{dAH} - \widehat{E}_{dBH}}{\Delta t_{hvvis}}, \quad (16)$$

363 which, in CAM-SE, includes a frictional heating term from viscosity on momentum

$$\partial\widehat{E}_{dyn}^{(fheat)} = \frac{\widehat{E}_{dAH} - \widehat{E}_{dCH}}{\Delta t_{hvvis}}, \quad (17)$$

364 where $\Delta t_{hvvis} = \frac{\Delta t_{phys}}{n_{split} \times r_{split} \times hypervis_subcycle}$ is the time step of the sub-stepped
 365 viscosity. The residual

$$\partial\widehat{E}_{dyn}^{(res)} = \partial\widehat{E}_{dyn}^{(2D)} - \partial\widehat{E}_{dyn}^{(hvvis)}, \quad (18)$$

366 is the energy error due to inviscid dynamics and time-truncation errors.

367 The energy tendency due to vertical remapping is

$$\partial\widehat{E}_{dyn}^{(remap)} = \frac{\widehat{E}_{dAR} - \widehat{E}_{dAD}}{\Delta t_{remap}}, \quad (19)$$

368 where $\Delta t_{remap} = \frac{\Delta t_{phys}}{n_{split}}$.

369 The 3D adiabatic dynamical core (no physics forcing but including friction) energy
 370 tendency is denoted

$$\partial\widehat{E}_{dyn}^{(adiab)} = \partial\widehat{E}_{dyn}^{(2D)} + \partial\widehat{E}_{dyn}^{(remap)}. \quad (20)$$

- 371 5. $\partial\widehat{E}^{(pdc)}$: Total spurious energy tendency due to physics-dynamics coupling errors is
 372 the difference between the energy tendency from physics and the energy tendency
 373 in the dynamics resulting from adding the physics increment to the dynamical core
 374 state

$$\partial\widehat{E}^{(pdc)} = \partial\widehat{E}_{phys}^{(phys)} - \partial\widehat{E}_{dyn}^{(phys)} \text{ assuming } \partial\widehat{E}^{(discr)} = 0, \quad (21)$$

375 where

$$\partial\widehat{E}_{dyn}^{(phys)} = \frac{\widehat{E}_{dBd} - \widehat{E}_{dAF}}{\Delta t_{pdc}}, \quad (22)$$

376 and Δt_{pdc} is the time-step between physics increments being added to the dynami-
 377 cal core. Remember we are dealing with average rates so terms computed with dif-
 378 ferent time steps can be compared, but differences cannot be taken between terms
 379 sampled with different time steps.

The physics-dynamics coupling TE tendency $\partial\widehat{E}^{(pdc)}$ makes use of TE formulas in dynamics and in physics so (21) is only well-defined if the TE formula discrepancy is zero, $\partial\widehat{E}^{(discr)} = 0$. As mentioned in Section 2.1, CAM-SE has the option to switch the continuous equations of motion conserving the TE used by CAM physics (8) instead of the more comprehensive TE formula (7).

In CAM-SE there are 3 physics-dynamics coupling algorithms described in detail in section 3.6 in *Lauritzen et al. [2018]* and reviewed in the introduction here. One is *state-update* in which the entire physics increments are added to the dynamics state at the beginning of dynamics (referred to as `ftype=1`), in which case $\Delta t_{pdc} = \Delta t_{phys}$. Another is *dribbling* in which the physics tendency is split into `nsplit` equal chunks and added throughout dynamics (more precisely after every vertical remapping; referred to as `ftype=0` resulting in $\Delta t_{pdc} = \frac{1}{nspit}\Delta t_{phys}$), and then a *combination* of the two (referred to as `ftype=2`) where tracers (mass variables) use *state-update* (`ftype=1`) and all other physics tendencies use *dribbling* (`ftype=0`).

6. $\partial\widehat{E}^{(efix)}$: Global energy fixer tendency, defined in (14), is applied at the beginning of the parameterizations. The correction needed is the global average difference between the state passed from the dynamics and the state that was saved after the physics updated the state but before the dry mass correction. It includes all spurious sources from the dry mass correction, remappings between physics and dynamics, dynamical core, differing energy definitions (if present), hyperviscosity, and vertical remapping.

2.5 A few observations regarding the energy budget terms

It is useful to note that the energy fixer ‘fixes’ energy errors for the dynamical core, pressure work **error**, physics-dynamics coupling and TE discrepancy

$$-\partial\widehat{E}_{phys}^{(efix)} = \partial\widehat{E}_{phys}^{(pwork)} + \partial\widehat{E}_{dyn}^{(adiab)} + \partial\widehat{E}^{(pdc)} + \partial\widehat{E}^{(discr)}. \quad (23)$$

The forcing from the parameterizations, $\partial\widehat{E}_{phys}^{(param)}$, does not appear in this budget (although the dynamical core state does ‘feel’ the parameterization forcing) as the energy cycle for the parameterizations is, by design in CAM, closed (balanced by fluxes in/out of the physics columns). If $\partial\widehat{E}^{(discr)} = 0$, one can use (23) to diagnose energy dissipation in the dynamical core and physics-dynamics coupling from quantities computed only in physics

$$\partial\widehat{E}_{dyn}^{(adiab)} + \partial\widehat{E}^{(pdc)} = -\partial\widehat{E}_{phys}^{(efix)} - \partial\widehat{E}_{phys}^{(pwork)} \text{ for } \partial\widehat{E}^{(discr)} = 0. \quad (24)$$

This is useful if the diagnostics are not implemented in the dynamical core; in particular, if the *state-update* (`ftype=1`) physics-dynamics coupling method is used then $\partial\widehat{E}^{(pdc)} = 0$ and the TE errors in the dynamical core can be computed without diagnostics implemented in the dynamical core. Also, (24) provides an alternative formula for $\partial\widehat{E}^{(pdc)}$ compared to (21):

$$\partial\widehat{E}^{(pdc)} = -\partial\widehat{E}_{phys}^{(efix)} - \partial\widehat{E}_{phys}^{(pwork)} - \partial\widehat{E}_{dyn}^{(adiab)} \text{ assuming } \partial\widehat{E}^{(discr)} = 0. \quad (25)$$

If $\partial\widehat{E}^{(pdc)} = 0$ (23) can be used to compute $\partial\widehat{E}^{(discr)}$

$$\partial\widehat{E}^{(discr)} = -\partial\widehat{E}_{phys}^{(efix)} - \partial\widehat{E}_{phys}^{(pwork)} - \partial\widehat{E}_{dyn}^{(adiab)}, \text{ assuming } \partial\widehat{E}^{(pdc)} = 0. \quad (26)$$

Note that we can not use (21) to compute $\partial\widehat{E}^{(discr)}$ since $\widehat{E}_{phys} \neq \widehat{E}_{dyn}$.

3 Results

A series of simulations have been performed with CESM2.1 using CAM version 6 (CAM6) physics (<https://doi.org/10.5065/D67H1H0V>) on NCAR’s Cheyenne cluster [*Computational and Information Systems Laboratory, 2017*]. All simulations are at nominally $\sim 1^\circ$ horizontal resolution (for CAM-SE that is 30×30 elements on each cubed-sphere face and for CAM-FV its 192×288 latitudes-longitudes) and using the standard

Table 1. TE tendencies in units of W/m^2 associated with various aspects of CAM-SE run in AMIP-type setup (unless otherwise noted). Column 1 is the identifier for the model configuration. See the text for a brief summary of these descriptors. They are defined in more detail in the following sections where the section titles also include the ‘Descriptor’ from Table 1 to make it easier for the reader to match Table entries with discussion in the text. Column 2 is \mathcal{N} =qsize_condensate_loading identifying how many water species are thermodynamically/inertially active in the dynamical core (see section 2.1 for details). Column 3, lcp_moist, indicates whether or not the heat capacity includes water variables or not and column 4 shows physics-dynamics coupling method ftype. The TE tendencies $\partial \widehat{E}$ in columns 5-14 are defined in section 2.4. If $\partial \widehat{E}$ is less than $10^{-5} W/m^2$ it is set to zero in the Table. Significant changes compared to the baseline (TE consistent configuration) discussed in the main text are in bold font. Entries marked with ‘-’ refer to TE tendencies that can not be directly calculated with the current framework.

Descriptor	\mathcal{N}	lcp_moist	ftype	$\partial \widehat{E}_{phys}^{(pwork)}$	$\partial \widehat{E}_{phys}^{(fix)}$	$\partial \widehat{E}_{phys}^{(discr)}$	$\partial \widehat{E}_{dyn}^{(2D)}$	$\partial \widehat{E}_{dyn}^{(heat)}$	$\partial \widehat{E}_{dyn}^{(res)}$	$\partial \widehat{E}_{dyn}^{(remap)}$	$\partial \widehat{E}_{dyn}^{(adiab)}$	$\partial \widehat{E}^{(pdc)}$
<i>TE consistent</i>	1	false	1	0.312	0.300	0	-0.601	-0.608	0.565	0.007	-0.011	-0.613
‘dribbling’ A	1	false	0	0.315	0.313	0	-0.577	-0.584	0.568	0.007	-0.011	-0.588
‘dribbling’ B	1	false	2	0.316	0.341	0	-0.598	-0.606	0.563	0.008	-0.011	-0.609
vert limiter	1	false	1	0.317	0.472	0	-0.590	-0.597	0.509	0.006	-0.199	-0.789
smooth topo	1	false	1	0.315	-0.008	0	-0.295	-0.300	0.493	0.005	-0.012	-0.307
energy discr	5	true	1	0.332	-0.313	0.594	-0.603	-0.612	0.575	0.009	-0.011	-0.614
default	5	true	2	0.316	-0.272	-	-0.578	-0.587	0.579	0.010	-0.012	-0.589
<i>QPC6</i>	1	false	1	0.305	-0.169	0	-0.129	-0.131	0.477	0.001	-0.007	-0.136
<i>FHS94</i>	1	false	2	-	-	-	-0.025	-0.025	0.122	0	0.005	-0.020
<i>FV</i>	1	false	1	0.304	0.670	0	-	-	-	-	-	-0.974
<i>CSLAM</i>	1	false	1	0.312	0.239	0	-0.547	-0.557	0.620	0.010	-0.011	-0.558
<i>CSLAM default</i>	5	true	2	0.320	-0.342	-	-0.524	-0.537	0.641	0.013	-0.011	-0.535

423 32 levels in the vertical. Unless otherwise noted all simulations are 13 months in dura-
 424 tion and the last 12 months are used in the analysis. Total energy budgets are summarized
 425 in Table 1 and discussed below. The first column gives identifying ‘Descriptors’ which
 426 are briefly summarized below and defined in more detail in the following sections. The
 427 section titles also include the ‘Descriptor’ from Table 1 to make it easier for the reader
 428 to match Table entries with discussion in the text. Important changes to TE errors are
 429 marked with bold font in Table 1.

430 Various configurations are used and referred to in terms of the *COMPSET* (Com-
 431 ponent Set) value used in CESM2.1 The *COMPSET F2000climo* configuration refers
 432 to ‘real-world’ AMIP (Atmospheric Model Intercomparison Project) type simulations us-
 433 ing perpetual year 2000 SST (Sea Surface Temperature) boundary conditions. The first 7
 434 simulations in the table (those above the horizontal line) are such AMIP-type simulations
 435 (*F2000climo*) with the first serving as a control for the 6 following variants. The remain-
 436 ing 5 simulation descriptors (below the horizontal line in Table 1) list their *COMPSET* or
 437 dynamical core settings.

438 The different configurations listed below are chosen to assess different aspects of the
 439 dynamical core numerical algorithm, PDC method, surface conditions, etc. (pointed out in
 440 parenthesis at the end of each item listing) on the TE budget:

- 441 • *TE consistent*: The TE consistent version uses *state update* physics-dynamics cou-
 442 pling (*ftype* 1) described in section 3.1 (this configuration does not have PDC
 443 errors and the same TE definition in physics and dynamics; and hence the ene-
 444 getically most consistent setup),
- 445 • ‘*dribbling*’ A: as *TE consistent* but with *dribbling* physics-dynamics coupling (*ftype*
 446 0) (section 3.2; this setup is used to assess PDC errors),
- 447 • ‘*dribbling*’ B: as *TE consistent* but with *dribbling* combination physics-dynamics
 448 coupling (*ftype* 2) (section 3.2; this setup is used to assess PDC errors),
- 449 • *vert limiter*: as *TE consistent* but using limiters in the vertical remapping of mo-
 450 mentum (section 3.3; experiment used to assess TE errors associated with shape-
 451 preserving limiters in vertical remapping),
- 452 • *smooth topo*: as *TE consistent* but using smoother topography (see section 3.4 experiment
 453 used to assess TE sensitivity to surface roughness),
- 454 • *energy discr*: The version with energy discrepancy (but no physics-dynamics cou-
 455 pling errors) described in section 3.5 (experiment used to estimate energy discrep-
 456 ency errors),
- 457 • *default*: as *energy discr* version but with *ftype*=2 which is the current default
 458 CAM-SE (section 3.5; we assess this configuration as it is the default CAM-SE
 459 configuration),
- 460 • *QPC6*: A simplified aqua-planet setup based on the *TE consistent*, i.e an aqua-
 461 planet setup using CAM6 physics; an ocean covered planet in perpetual equinox,
 462 with fixed, zonally symmetric sea surface temperatures [Neale and Hoskins, 2000;
 463 Medeiros et al., 2016] (section 3.6; experiment use to assess TE errors in a simpli-
 464 fied moist environment),
- 465 • *FSH94*: Dry dynamical core configuration based on Held-Suarez forcing which re-
 466 laxes temperature to a zonally symmetric equilibrium temperature profile and sim-
 467 ple linear drag at the lower boundary [Held and Suarez, 1994] (section 3.7; experi-
 468 ment used to assess if TE errors in on of the simplest climate test cases is represen-
 469 tative of full model TE errors),,
- 470 • *FV*: A configuration with the SE dynamical core replaced with the finite-volume
 471 core (section 3.8 experiment used to assess TE errors of the ‘workhorse’ dynamical
 472 core for CMIP6 simulations), and

- 473 • *CSLAM*: The quasi equal-area physics grid configuration of CAM-SE based on the
 474 TE consistent setup (section 3.9; used to assess TE errors associated with separating
 475 the dynamics grid from the physics grid)
 476 • *CSLAM default*: Same as *CSLAM* configuration but with `ftype=2` and all forms
 477 of water thermodynamically/inertially active in the dynamical core (setup evaluated
 478 since it is the default CAM-SE-CSLAM setup).

485 **3.1 TE consistent: state-update physics-dynamics coupling (`ftype=1`) and no TE
 486 formula discrepancy**

487 This configuration is the most energetically consistent in that the physical parametrizations and the continuous equations of motion on which the dynamical core is based,
 488 conserve the same TE (defined in equation (8)); and there are no spurious sources/sinks in
 489 physics-dynamics coupling. Energetic consistency in dynamics and physics is obtained
 490 by setting $c_p^{(\ell)} \equiv c_p^d$ and $\mathcal{L}_{all} = \{d, wv\}$ in the dynamical core equations of motion and TE computations. Associated namelist changes resulting in this configuration are
 491 `lcp_moist = .false.`, `se_qsize_condensate_loading = 1`, and `ftype = 1`.

494 The TE consistent configuration in AMIP-type simulation (*F2000climo*) is used to
 495 compute baseline TE tendencies which will be used to compare with other model configura-
 496 tions. First we establish how long an average is needed to get robust TE tendency
 497 estimates. Figure 2 shows $\partial\widehat{E}$ for various aspects of CAM-SE as a function of time. The
 498 simulation length is 5 years and monthly average values are used for the analysis. First
 499 consider the left plot. The TE tendency from parameterizations ($\partial\widehat{E}_{phys}^{(param)}$) show signif-
 500 icant variability with an amplitude of approximately $2.5W/m^2$. As noted above this term
 501 does not figure in the spurious TE budget. The net source/sink provides an equal and op-
 502 posite term to balance it. That said, the variability is reflected onto the TE tendency due
 503 to pressure work **error** $\partial\widehat{E}_{phys}^{(pwork)} \approx 0.32 \pm 0.08W/m^2$. On the scale used in the left-
 504 hand plot the TE tendency of the adiabatic dynamical core $\partial\widehat{E}_{dyn}^{(adiab)}$ does not seem to be
 505 affected by $\partial\widehat{E}_{phys}^{(param)}$ or $\partial\widehat{E}_{phys}^{(pwork)}$ in terms of variability, and remains stable at approxi-
 506 mately $-0.6W/m^2 \pm 0.02W/m^2$. The TE fixer, in this model configuration, fixes $\partial\widehat{E}_{dyn}^{(adiab)}$
 507 and $\partial\widehat{E}_{phys}^{(pwork)}$. Since the TE imbalance in the adiabatic dynamics remains approximately
 508 constant and the TE tendency associated with pressure work **error** has variability, the TE
 509 tendency from the $\partial\widehat{E}_{phys}^{(efix)}$ has variability; $\partial\widehat{E}_{phys}^{(efix)} \approx 0.30 \pm 0.08W/m^2$. As a consistency
 510 check $-\partial\widehat{E}_{dyn}^{(adiab)} - \partial\widehat{E}_{phys}^{(pwork)}$ is plotted with asterisk's and they coincide (as expected)
 511 with $\partial\widehat{E}_{phys}^{(efix)}$ fulfilling (23).

512 The right-hand plot in Figure 2 shows a breakdown of the dynamical core TE ten-
 513 dencies. The majority of the TE errors are due to hyperviscosity on temperature and pres-
 514 sure, $\partial\widehat{E}_{dyn}^{(hvis)} \approx -0.61 \pm 0.01W/m^2$. The diffusion of momentum is added back as fric-
 515 tional heating and is therefore not part of $\partial\widehat{E}_{dyn}^{(hvis)}$. The frictional heating is a significant
 516 term in the TE tendency budget $\partial\widehat{E}_{dyn}^{(fheat)} \approx 0.56 \pm 0.02W/m^2$ and exhibits some variabil-
 517 ity but with a rather small amplitude. The remaining TE error in the floating Lagrangian
 518 dynamics is inviscid dissipation and time-truncation errors $\partial\widehat{E}_{dyn}^{(res)} = \partial\widehat{E}_{dyn}^{(2D)} - \partial\widehat{E}_{dyn}^{(hvis)} \approx$
 519 $0.007W/m^2$. The TE tendency from vertical remapping is approximately $\partial\widehat{E}_{dyn}^{(remap)} \approx$
 520 $-0.01W/m^2$. To within $\sim 0.02W/m^2$ the dynamical core TE tendency terms can be com-
 521 puted from just one month average TE integrals. The TE tendencies computed in physics,
 522 excluding $\partial\widehat{E}_{phys}^{(param)}$, exhibit more variability and are only accurate to $\sim 0.1W/m^2$ after a
 523 one month average.

526 While it is advantageous to use *state-update* physics-dynamics coupling algorithm
 527 (`ftype=1`) in terms of having no spurious TE tendency from coupling, $\partial\widehat{E}^{(pdc)} = 0$,
 528 it does result in spurious gravity waves in the simulations [see, e.g., Figure 5 in *Gross*

et al., 2018]. Figure 3a shows a 1 year average of $|\frac{dp_s}{dt}|$, a measure of high frequency gravity wave noise. It clearly exhibits unphysical oscillations coinciding with element boundaries. Details of the spectral-element method, its coupling to physics and associated noise issues are discussed in detail in Herrington et al. [2018]. The noise in the solutions is even visible in the 500hPa pressure velocity annual average (Figure 4a). This issue can be alleviated by using a shorter physics time-step so that the physics increments are smaller (not shown). Climate modelers have historically not pursued a shorter physics time-step in production configurations as climate parameterizations are computationally expensive and there is a large sensitivity to physics time-steps in the simulated climate [e.g. Williamson and Olson, 2003; Wan et al., 2015].

539 3.2 ‘dribbling’ A/B: Non-TE conservative physics-dynamics coupling (`ftype=0`, 2)

540 Before discussing the impact of different PDC methods on the TE budget, we dis-
 541 cuss element boundary noise issues in CAM-SE which are related to PDC method. This
 542 motivates the different PDC methods implemented in CAM-SE.

543 3.2.1 Spurious element boundary noise from physics-dynamics coupling

544 When switching to *dribbling* physics-dynamics coupling algorithm (`ftype=0`) in
 545 which the tendencies from physics are added throughout the dynamics (in this case twice
 546 per physics time-step) then the noise issues described in previous section disappear (Figure
 547 3b and 4b). That said, there is a significant issue with this approach; the tracer mass bud-
 548 get may not be closed. How this comes about is illustrated in Figure 5 and explained in
 549 the next paragraph.

550 The orange curve on Figure 5a, b, d, and e is the initial state of, e.g., cloud liq-
 551 uid mixing ratio as a function of location, e.g., longitude. Cloud liquid is zero outside
 552 of clouds and hence provides a good example for the purpose of this illustration. The
 553 light blue arrows show the increments (in terms of length of arrow) computed by the
 554 parameterizations based on the initial state and scaled for the partial update with *dribbling*
 555 (`ftype=0`). With *state-update* (`ftype=1`) the increments from physics are added to the
 556 dynamical core state (dotted line on 5b) before the dynamical core advances the solution
 557 in time. The parameterizations are designed to not drive the mixing ratios negative so the
 558 state-update in dynamics will not generate negatives (or overshoots). Then the dynami-
 559 cal core advects the distribution (solid curve on Figure 5c). With *dribbling* (`ftype=0`) the
 560 physics increments are split into equal chunks (in this illustration two; blue errors on Fig-
 561 ure 5d). Half of the physics increments are added to the initial state (dotted line on Fig-
 562 ure 5e) and then dynamics advects the distribution half of the total dynamical core steps
 563 (dashed line on Figure 5e). Then the other half of the physics increments are applied (in
 564 the same location as they were computed by physics). Now after the previous/first advec-
 565 tion step the cloud liquid distribution has moved and the mixing ratio may be zero (or
 566 less than the increment prescribed by physics) where the physics forcing is applied (e.g.,
 567 left side of dashed curve). Hence the physics increment is driving the mixing ratios neg-
 568 ative in those locations. Thereafter the distribution is advected (solid curve on Figure 5f).
 569 In CAM the increments added in the dynamical core are limited so that they drive the
 570 mixing to zero (but not negative) if this problem occurs. This leads to a net source of
 571 mass compared to the mass change that the parameterizations prescribe (see Figure 6).
 572 Although the average source of mass is small each time-step it always has the same sign
 573 (i.e. it is a bias) and therefore accumulates. Zhang et al. [2017] estimated that this spuri-
 574 ous source of mass is equivalent to $\sim 10\text{cm}$ sea-level rise per decade in coupled climate
 575 simulation experiments.

576 The majority of the noise with *state-update* (`ftype=1`) physics-dynamics coupling
 577 method comes from momentum sources/sinks and heating/cooling. A way to alleviate
 578 noise problems and, at the same time, close the tracer mass budgets (in physics-dynamics

coupling) is to use *state-update* (`ftype=1`) coupling for tracers and *dribbling* (`ftype=0`) coupling for momentum and temperature (referred to as *combination*, `ftype=2`). Figure 3c shows the noise diagnostic $|\frac{dp_s}{dt}|$ for *combination* (`ftype=2`) coupling. Figure 3c looks very similar to Figure 3b but there is some noise near element boundaries. That said, in terms of vertical pressure velocities *combination* (`ftype=2`) and *dribbling* (`ftype=0`) climates are similar in terms of the level of noise (Figure 4b and 4c). The element noise in CAM-SE with *combination* (`ftype=2`) seen in both $|\frac{dp_s}{dt}|$ and 500hPa pressure velocity can be ‘removed’ by using CAM-SE-CSLAM (Figure 3d) which uses a quasi equal-area physics grid and CSLAM [Conservative Semi-Lagrangian Multi-tracer; *Lauritzen et al.*, 2010] consistently coupled to the SE method [*Lauritzen et al.*, 2017]. The noise patterns in vertical velocity off the western coast of South America are present in all CAM-SE simulations (and hence not related to physics-dynamics coupling algorithm) are also ‘removed’ by using CAM-SE-CSLAM [*Herrington et al.*, 2018].

592 3.2.2 Spurious TE tendencies from physics-dynamics coupling

593 When using the same TE formula in the dynamical core and physics the spurious
 594 TE tendency from physics-dynamics coupling can be assessed. As described in item 5
 595 (Section 2.3), PDC errors can be attributed to underlying pressure changes during the
 596 ‘dribbling’ of temperature and velocity component increments as well as PDC ‘clipping’
 597 errors in the water variables (the process in which ‘clipping’ occurs is described in detail
 598 in the previous subsection). The TE error associated with ‘clipping’ PDC error occurs due
 599 to the mass-change prescribed by physics consistent with the fluxes in/out of the physics
 600 column does not equal the actual mass change applied to the dynamical core state due to
 601 ‘clipping’

602 For `ftype=2` PDC only the increment for temperature and momentum are *dribbled*
 603 whereas tracer mass is state-updated (no ‘clipping’ errors). This results in a spurious PDC
 604 TE tendency of $\partial\widehat{E}^{(pdc)} = -0.484W/m^2$. When using `ftype=0` PDC also tracer increments
 605 are *dribbled* (hence there are ‘clipping’ PDC errors) a similar TE tendency results
 606 $\partial\widehat{E}^{(pdc)} = -0.469W/m^2$. The difference between the TE PDC tenendency for `ftype=2`
 607 and `ftype=0` provides an estimate of the TE PDC ‘clipping’ error. The ‘clipping’ PDC
 608 TE tendency is very small $0.015W/m^2$.

609 3.3 vert limiter: Limiters on vertical remapping of momentum

610 CAM-SE uses a floating Lagrangian vertical coordinate [*Starr*, 1945; *Lin*, 2004]
 611 which requires the remapping of the atmospheric state from floating levels back to refer-
 612 ence levels to maintain computational stability and to provide state data consistent with
 613 the physics formulation. The mapping algorithm is based on the mass conservative PPM
 614 (Piecewise Parabolic Method) with options for shape-preserving limiters. In CAM-SE mo-
 615 mentum components and internal energy are used as the variables mapped in the vertical
 616 [*Lauritzen et al.*, 2018] and, contrary to earlier versions of CAM-SE, there is no limiter
 617 on the remapping of wind components. If the shape-preserving limiter is used for mo-
 618 mentum mapping then the TE dissipation increases by over an order of magnitude from
 619 $\sim 0.01W/m^2$ to $\sim 0.2W/m^2$ (Table 1).

620 3.4 smooth topo: Smoother topography

621 Topography for CAM is generated using a new version of the software/algorithm de-
 622 scribed in *Lauritzen et al.* [2015] that is available at <https://github.com/NCAR/Topo>.
 623 The updates to the software includes smoothing algorithms and the computation of sub-
 624 grid-scale orientation of topography.

625 The default topography in CAM-SE uses the same amount of topography smooth-
 626 ing as CAM-FV (distance weighted smoother applied to the raw topography on $\sim 3\text{km}$

627 cubed-sphere grid with a smoothing radius of 180km referred to as C60). When the to-
 628 topography is smoother (in this case using C92 smoothing, i.e. smoothing radius of approx-
 629 imately 276km) the hyperviscosity operators are less active leading to reduced TE errors,
 630 i.e. $\partial\widehat{E}_{dyn}^{(hvis)}$ is reduced in half from approximately $-0.6W/m^2$ to $-0.3W/m^2$. The vertical
 631 remapping TE error, however, remains approximately the same. Since the pressure work
 632 **error** is approximately $0.3W/m^2$ it almost exactly compensates for the TE tendency from
 633 the dynamical core $\partial\widehat{E}_{dyn}^{(adiab)}$. Hence if one would only diagnose the TE tendency from
 634 the energy fixer one could mistakenly conclude that the model universally conserves TE
 635 when, in fact, there are compensating TE errors in the system. These compensating errors
 636 can only be diagnosed through a careful breakdown of the total TE tendencies.

637 3.5 default: TE formula discrepancy errors

638 To assess the TE errors due to the discrepancy in the energy formula used by dy-
 639 namics and physics, a simulation using *state-updating* (*ftype*=1, no ‘dribbling’ errors) and
 640 thermodynamically/inertially active condensates in the dynamical core (*qsize_condensate_loading* =
 641 5) and consistent/accurate associated heat capacities $c_p^{(\ell)}$ (namelist *lcp_moist=true.*)
 642 has been performed. In this setup the continuous equations of motion in the dynami-
 643 cal core conserve an energy different from physics, and the energy fixer will restore the
 644 ‘physics’ version of energy. Despite the dynamical core now using a more comprehensive
 645 formula for energy, the TE dissipation terms in the dynamical core are roughly the same
 646 as in the energy consistent versions of the model. Using (26) we can assess the TE energy
 647 discrepancy errors which result in $\sim 0.59W/m^2$. *Taylor* [2011] found a similar result just
 648 from using the more comprehensive formula for heat capacity (based on dry air and water
 649 vapor) and not including thermodynamically/inertially active condensates. As noted before
 650 this formulation inconsistency is due to the evolutionary nature of CAM development and
 651 it is the intention to remove this inconsistency in future versions of the model.

652 The default version of CAM-SE uses this configuration but with *combination* (*ftype*=2)
 653 which has similar TE characteristics (see Table 1). That said, the physics-dynamics cou-
 654 pling error from *dribbling* momentum and temperature tendencies and the energy discrep-
 655 ancies errors can not be separated in this configuration:

$$\partial\widehat{E}^{(pdc)} + \partial\widehat{E}^{(discr)} = 0.546W/m^2, \quad (27)$$

656 using (23). With *state-updating* (*ftype*=1) (i.e. $\partial\widehat{E}^{(pdc)} = 0$) the energy discrepancy error
 657 was $0.594W/m^2$ and in the energy consistent setup (i.e. $\partial\widehat{E}^{(discr)} = 0$) but using *dribbling*
 658 (*ftype*=2) we got $\partial\widehat{E}^{(pdc)} = 0.484W/m^2$. So if the physics-dynamics coupling errors
 659 and energy discrepancy errors in the different configurations would be additive, one would
 660 have expected $\partial\widehat{E}^{(pdc)} + \partial\widehat{E}^{(discr)}$ to be over $1W/m^2$ which is clearly not the case (27).
 661 Again, it must be concluded that there are canceling errors in the system.

662 3.5.1 2D structure of TE errors

663 Figure 7 shows the two-dimensional spatial structure of column-integrated TE ten-
 664 dencies for the *default* configuration. The first plot (Figure 7a) shows column inte-
 665 grated $\partial E^{(param)}$, i.e. the spatial structure of ‘physical’ TE tendency. Only contours from
 666 $\pm 150W/m^2$ are shown although the actual range (noted above color bar) is $-148.3W/m^2$ to
 667 $1770W/m^2$. The larger positive values are only for a small number of grid points (moun-
 668 tains of New Guinea). The column-integrated dynamical core TE tendency $\partial\widehat{E}^{(adiab)}$
 669 (Figure 7c) approximately balances $\partial E^{(param)}$. The TE pressure work error tendency
 670 $\partial E^{(pwork)}$ (Figure 7b) is, as expected, largest where precipitation and evaporation is largest.
 671 The last 3 plots show terms in the dynamical core budget: column-integrated TE ten-
 672 dency for hyperviscosity, $\partial\widehat{E}^{(hvis)}$, vertical remapping, $\partial\widehat{E}^{(remap)}$, and frictional heating,
 673 $\partial\widehat{E}^{(heat)}$. Compared to $\partial E^{(param)}$ the hyperviscosity tendencies $\partial\widehat{E}^{(hvis)}$ are very large
 674 meaning that the frictionless adiabatic dynamical core creates very large TE tendencies
 675 (not shown) that are, to a large degree, compensated for by the hyperviscosity operators.

Otherwise the total dynamical core TE tendencies would be equally large. The frictional heating TE tendency is largest over/near topography. Similarly for vertical remapping but, in addition, there are large TE tendencies in areas of large updrafts/downdrafts over ocean.

3.6 QPC6: Simplified surface

By running the model in aqua-planet configuration one can assess the effect of simplifying the surface boundary condition. In particular, without topography forcing the dynamical core is not challenged with respect to stationary near-grid-scale forcing. The TE tendency with respect to pressure work **error** remains the same $\partial\widehat{E}_{phys}^{(pwork)}$ as the AMIP-type simulations, however, the adiabatic dynamical core TE tendency reduces to $\partial\widehat{E}_{dyn}^{(adiab)} = -0.14W/m^2$ (approximately a factor 4 reduction). Most of that reduction is due to viscosity $\partial\widehat{E}_{dyn}^{(hvis)} = -0.13W/m^2$. The frictional heating is roughly the same as AMIP $\partial\widehat{E}_{dyn}^{(fheat)} = 0.48W/m^2$ as is the vertical remapping $\partial\widehat{E}_{dyn}^{(remap)} = -0.01W/m^2$. To evaluate the dynamical cores diffusion of TE it is therefore important to asses the model in a configuration with topography as the wave dynamics generated by topography leads to more active diffusion operators.

3.7 FHS94: Simplified physics (no moisture)

Simplifying the setup even further by replacing the parameterizations with relaxation towards a zonally symmetric temperature profile and simple boundary layer friction (Held-Suarez forcing) as well as excluding moisture, the TE errors in the dynamical core decreases even further to $\sim 0.002W/m^2$ since there is no small scale forcing. Small scales are only created by the nonlinear dynamics and the physics works to damp them. Hyper-viscosity is less active leading to significant reductions compared to aqua-planet and ‘real-world’ simulation results. The TE diffusion in vertical remapping reduces by an order of magnitude compared to the aqua-planet simulations ($\sim 0.0005W/m^2$). This further emphasizes that TE diffusion assessment in a simplified setup is not necessarily telling for the dynamical cores performance with moist physics and topography that challenge the dynamical core in terms of strong grid-scale forcing.

3.8 FV: Changing dynamical core to Finite-Volume (FV)

As a comparison the TE error characteristics of the CAM-FV dynamical core are assessed. Although the TE diagnostics have not been implemented in the CAM-FV dynamical core, the TE diagnostics in CAM physics are independent of dynamical core and can therefore be activated with CAM-FV. The CAM-FV dynamical core uses *state-update* physics-dynamics coupling (*fctype*=1) ($\partial\widehat{E}^{(pdc)} = 0$) and the same TE definition as CAM physics ($\partial\widehat{E}^{(discr)} = 0$). Hence (24) can be used to compute the TE errors of the CAM-FV dynamical core, $\partial\widehat{E}_{dyn}^{(adiab)} \approx -1W/m^2$. As we do not have the **breakdown** of $\partial\widehat{E}_{dyn}^{(adiab)}$ it can not be determined how much of the TE errors are due to the vertical remapping. Furthermore, CAM-FV contains intrinsic dissipation operators (limiters in the flux operators) making it difficult to assess TE sources/sinks due to dissipation. Note that the pressure work **error** even with a change of dynamical core remains approximately the same as the CAM-SE configurations.

3.9 CSLAM: Quasi equal-area physics grid

This configuration was discussed in the context of element noise in section 3.2.1. By averaging the dynamics state of an equal-partitioning (in central angle cubed-sphere coordinates) of the elements, the element-boundary noise found in CAM-SE can be removed. Lauritzen *et al.* [2018] argue that this way of computing the state for the physics

727 is more consistent with physics in terms of providing a cell-averaged state instead of ir-
 728 regularly spaced point (quadrature) values. In order to achieve a closed mass-budget, this
 729 configuration uses CSLAM for tracer transport rather than SE transport. That said, the
 730 physics columns no longer coincide with the quadrature grid and there are TE errors asso-
 731 ciated with mapping state and tendencies between the two grids.

732 In this configuration the energy diagnostics computed in the dynamical core are
 733 computed on the quadrature grid and the energy diagnostics computed in physics are on
 734 the physics grid. If the TE consistent configuration is used (`ftype=1, qsize_condensate_loading=1,`
 735 `lcp_moist=.false.`) then the physics-dynamical coupling errors, $\widehat{E}^{(pdc)}$ computed with
 736 (21), are entirely due to mapping state from quadrature grid to physics grid and map-
 737 ping tendencies back the quadrature grid from the physics grid. The results is $\widehat{E}^{(pdc)} =$
 738 $-0.07W/m^2$ which is a rather small error compared to other terms in the TE budget.

739 Due to similar noise problems with CAM-SE-CSLAM when using `ftype=1` that
 740 were observed in CAM-SE (Figure 3 and 4), the default version of CAM-SE-CSLAM uses
 741 `ftype=2`. Again physics-dynamics coupling errors and TE discrepancy errors can not be
 742 separated; $\partial\widehat{E}^{(pdc)} + \partial\widehat{E}^{(discr)} = 0.557W/m^2$.

743 4 Conclusions

744 A detailed total energy (TE) error analysis of the Community Atmosphere Model
 745 (CAM) using version 6 physics (included in the CESM2.1 release) running at approxi-
 746 mately 1° horizontal resolution has been presented. In the global climate model there can
 747 be many spurious contributions to the TE budget. These errors can be divided into four
 748 categories: physical parameterizations, adiabatic dynamical core, the coupling between
 749 physics and dynamics, and TE definition discrepancies between dynamics and physics.
 750 The latter is not by design but through the evolutionary nature of model development. By
 751 capturing the atmospheric state at various locations in the model algorithm, a detailed
 752 budget of TE errors can be constructed. The net spurious TE energy errors are compen-
 753 sated with a global energy fixer (providing a global uniform temperature increment) every
 754 physics time-step.

755 In CAM physics the parameterizations have, by design, a closed energy budget (change
 756 in TE is balanced by fluxes in/out the top and bottom of physics columns) if it is assumed
 757 that pressure is not modified. However, the pressure changes due to fluxes of mass (e.g.,
 758 water vapor) in/out of the column which changes energy (referred to as pressure work
 759 **error**). The pressure work **error** with the full moist physics configuration is very stable
 760 across different configurations at $\sim 0.3W/m^2$. The TE errors in the spectral element (SE)
 761 dynamical core varies across configurations. Aspects that influence TE is the presence
 762 of topography, the amount of topography smoothing and moist physics. By smoothing
 763 topography more the TE error is cut in half from $\sim -0.6W/m^2$ to $\sim -0.3W/m^2$; and re-
 764 duces by a factor of **six** ($\sim -0.1W/m^2$) if no topography is present at all (aqua-planet
 765 configuration). Moist physics forcing also contributes significantly to the TE budget. For
 766 example, in the dry Held-Suarez setup TE dissipation of the SE dynamical core reduces
 767 to $-0.03W/m^2$. Topography and moist physics force the dynamical core at the grid scale
 768 and hence the viscosity operators are more active. Consistent with this statement is that
 769 the changes in TE discussed so far are almost entirely due to the viscosity operator TE
 770 dissipation. For CAM-SE the spurious TE dissipation in the adiabatic dynamical core is
 771 $\sim -0.6W/m^2$ in ‘real-world’ configurations. For comparison, CAM-FV’s spurious TE
 772 change due to the adiabatic dynamical core is $\sim -1W/m^2$.

773 By further breaking down the TE dissipation in the SE dynamical core it is ob-
 774 served the vertical remapping accounts for only $\sim -0.01W/m^2$. That said, if the shape-
 775 preserving limiters in the vertical remapping are invoked the TE dissipation increases 20-
 776 fold to $\sim -0.2W/m^2$. In CAM-SE the kinetic energy dissipation is added as heating in

777 the thermodynamic equation (also referred to as frictional heating). The frictional heat-
 778 ing remains very stable across configurations that include moisture ($\sim 0.5W/m^2$) and re-
 779 duces drastically for dry atmosphere setups (factor 4 reduction to ($\sim 0.12W/m^2$)). Hence
 780 this term is an important term in the TE budget. The TE budget for the dynamical core
 781 is dominated by TE change due to hyperviscosity; TE errors due to time-truncation and
 782 frictionless equations of motion are negligible. Errors associated with physics-dynamics
 783 coupling (if applicable) are approximately $0.5W/m^2$. Due to the evolutionary nature of
 784 model development the SE dynamical core's continuous equation of motion conserve a
 785 more comprehensive TE compared to the physical parameterizations. This TE discrep-
 786 ancies leads to an approximately $0.5W/m^2$ total energy source. Running physics on a dif-
 787 ferent grid than the dynamical introduces TE mapping errors such as in CAM-SE-CSLAM
 788 (Conservative Semi-Lagrangian Multi-tracer transport scheme). These errors are, however,
 789 rather small $-0.07W/m^2$.

790 A purpose of this paper is to better understand the energy characteristics of CAM
 791 and to encourage modeling groups to perform similar analysis to better understand the
 792 total energy flow in the atmospheric component of Earth system models. As has been
 793 demonstrated in this paper there can easily be compensating errors in the system which
 794 can not be identified without a detailed TE analysis.

795 Acknowledgments

796 The National Center for Atmospheric Research is sponsored by the National Science Foun-
 797 dation. Computing resources (doi:10.5065/D6RX99HX) were provided by the Climate
 798 Simulation Laboratory at NCAR's Computational and Information Systems Laboratory,
 799 sponsored by the National Science Foundation and other agencies. The data used to per-
 800 form the energy analysis can be found at [https://github.com/PeterHjortLauritzen/](https://github.com/PeterHjortLauritzen/2018-JAMES-energy)
 801 2018-JAMES-energy.

802 References

- 803 Boville, B. (2000), chap. Toward a complete model of the climate system in Numerical
 804 Modeling of the Global Atmosphere in the Climate System, pp. 419–442, Springer
 805 Netherlands.
- 806 Computational and Information Systems Laboratory (2017), Cheyenne: HPE/SGI ICE XA
 807 System (Climate Simulation Laboratory), Boulder, CO: National Center for Atmospheric
 808 Research, doi:10.5065/D6RX99HX.
- 809 Eldred, C., and D. Randall (2017), Total energy and potential enstrophy conserv-
 810 ing schemes for the shallow water equations using hamiltonian methods – part
 811 1: Derivation and properties, *Geosci. Model Dev.*, 10(2), 791–810, doi:10.5194/
 812 gmd-10-791-2017.
- 813 Gross, M., H. Wan, P. J. Rasch, P. M. Caldwell, D. L. Williamson, D. Klocke,
 814 C. Jablonowski, D. R. Thatcher, N. Wood, M. Cullen, B. Beare, M. Willett, F. Lemarié,
 815 E. Blayo, S. Malardel, P. Termonia, A. Gassmann, P. H. Lauritzen, H. Johansen, C. M.
 816 Zarzycki, K. Sakaguchi, and R. Leung (2018), Physics-dynamics coupling in weather,
 817 climate and earth system models: Challenges and recent progress, *Mon. Wea. Rev.*, 146,
 818 3505–3544, doi:10.1175/MWR-D-17-0345.1.
- 819 Held, I. M., and M. J. Suarez (1994), A proposal for the intercomparison of the dynamical
 820 cores of atmospheric general circulation models, *Bull. Amer. Meteor. Soc.*, 75, 1825–
 821 1830.
- 822 Herrington, A. R., P. H. Lauritzen, M. A. Taylor, S. Goldhaber, B. E. Eaton, K. A. Reed,
 823 and P. A. Ullrich (2018), Physics-dynamics coupling with element-based high-order
 824 Galerkin methods: quasi equal-area physics grid, *Mon. Wea. Rev.*
- 825 Jablonowski, C., and D. L. Williamson (2011), chap. The Pros and Cons of Diffusion,
 826 Filters and Fixers in Atmospheric General Circulation Models, pp. 381–493, Springer

- Berlin Heidelberg, Berlin, Heidelberg, doi:10.1007/978-3-642-11640-7_13.
- Kasahara, A. (1974), Various vertical coordinate systems used for numerical weather prediction, *Mon. Wea. Rev.*, 102(7), 509–522.
- Lauritzen, P. H., R. D. Nair, and P. A. Ullrich (2010), A conservative semi-Lagrangian multi-tracer transport scheme (CSLAM) on the cubed-sphere grid, *J. Comput. Phys.*, 229, 1401–1424, doi:10.1016/j.jcp.2009.10.036.
- Lauritzen, P. H., J. T. Bacmeister, T. Dubos, S. Lebonnois, and M. A. Taylor (2014), Held-Suarez simulations with the Community Atmosphere Model Spectral Element (CAM-SE) dynamical core: A global axial angular momentum analysis using Eulerian and floating Lagrangian vertical coordinates, *J. Adv. Model. Earth Syst.*, 6, doi: 10.1002/2013MS000268.
- Lauritzen, P. H., J. T. Bacmeister, P. F. Callaghan, and M. A. Taylor (2015), NCAR_Topo (v1.0): NCAR global model topography generation software for unstructured grids, *Geosci. Model Dev.*, 8(12), 3975–3986, doi:10.5194/gmd-8-3975-2015.
- Lauritzen, P. H., M. A. Taylor, J. Overfelt, P. A. Ullrich, R. D. Nair, S. Goldhaber, and R. Kelly (2017), CAM-SE-CSLAM: Consistent coupling of a conservative semi-lagrangian finite-volume method with spectral element dynamics, *Mon. Wea. Rev.*, 145(3), 833–855, doi:10.1175/MWR-D-16-0258.1.
- Lauritzen, P. H., R. Nair, A. Herrington, P. Callaghan, S. Goldhaber, J. Dennis, J. T. Bacmeister, B. Eaton, C. Zarzycki, M. A. Taylor, A. Gettelman, R. Neale, B. Dobbins, K. Reed, and T. Dubos (2018), NCAR release of CAM-SE in CESM2.0: A reformulation of the spectral-element dynamical core in dry-mass vertical coordinates with comprehensive treatment of condensates and energy, *J. Adv. Model. Earth Syst.*, doi: 10.1029/2017MS001257.
- Lin, S.-J. (2004), A 'vertically Lagrangian' finite-volume dynamical core for global models, *Mon. Wea. Rev.*, 132, 2293–2307.
- McRae, A. T. T., and C. J. Cotter (2013), Energy- and enstrophy-conserving schemes for the shallow-water equations, based on mimetic finite elements, *Quart. J. Roy. Meteor. Soc.*, 140(684), 2223–2234, doi:10.1002/qj.2291.
- Medeiros, B., D. L. Williamson, and J. G. Olson (2016), Reference aquaplanet climate in the community atmosphere model, version 5, *J. Adv. Model. Earth Syst.*, 8(1), 406–424, doi:10.1002/2015MS000593.
- Neale, R. B., and B. J. Hoskins (2000), A standard test for AGCMs including their physical parametrizations: I: the proposal, *Atmos. Sci. Lett.*, 1(2), 101–107, doi:10.1006/asle.2000.0022.
- Neale, R. B., C.-C. Chen, A. Gettelman, P. H. Lauritzen, S. Park, D. L. Williamson, A. J. Conley, R. Garcia, D. Kinnison, J.-F. Lamarque, D. Marsh, M. Mills, A. K. Smith, S. Tilmes, F. Vitt, P. Cameron-Smith, W. D. Collins, M. J. Iacono, R. C. Easter, S. J. Ghan, X. Liu, P. J. Rasch, and M. A. Taylor (2012), Description of the NCAR Community Atmosphere Model (CAM 5.0), *NCAR Technical Note NCAR/TN-486+STR*, National Center of Atmospheric Research.
- Skamarock, W. C., J. B. Klemp, M. G. Duda, L. Fowler, S.-H. Park, and T. D. Ringler (2012), A multi-scale nonhydrostatic atmospheric model using centroidal Voronoi tessellations and C-grid staggering, *Mon. Wea. Rev.*, 240, 3090–3105, doi:doi:10.1175/MWR-D-11-00215.1.
- Starr, V. P. (1945), A quasi-Lagrangian system of hydrodynamical equations., *J. Atmos. Sci.*, 2, 227–237.
- Taylor, M. A. (2011), Conservation of mass and energy for the moist atmospheric primitive equations on unstructured grids, in: P.H. Lauritzen, R.D. Nair, C. Jablonowski, M. Taylor (Eds.), Numerical techniques for global atmospheric models, *Lecture Notes in Computational Science and Engineering*, Springer, 2010, *in press.*, 80, 357–380, doi: 10.1007/978-3-642-11640-7_12.
- Thuburn, J. (2008), Some conservation issues for the dynamical cores of NWP and climate models, *J. Comput. Phys.*, 227, 3715–3730.

- 881 Trenberth, K. E., and J. T. Fasullo (2018), Applications of an updated atmospheric ener-
882 getics formulation, *J. Climate*, 31(16), 6263–6279, doi:10.1175/JCLI-D-17-0838.1.
- 883 Wan, H., P. J. Rasch, M. A. Taylor, and C. Jablonowski (2015), Short-term time step con-
884 vergence in a climate model, *J. Adv. Model. Earth Syst.*, 7(1), 215–225, doi:10.1002/
885 2014MS000368.
- 886 Williamson, D. L. (2002), Time-split versus process-split coupling of parameterizations
887 and dynamical core, *Mon. Wea. Rev.*, 130, 2024–2041.
- 888 Williamson, D. L., and J. G. Olson (2003), Dependence of aqua-planet simulations on
889 time step, *Q. J. R. Meteorol. Soc.*, 129(591), 2049–2064.
- 890 Williamson, D. L., J. G. Olson, C. Hannay, T. Toniazzo, M. Taylor, and V. Yudin (2015),
891 Energy considerations in the community atmosphere model (cam), *J. Adv. Model. Earth
892 Syst.*, 7(3), 1178–1188, doi:10.1002/2015MS000448.
- 893 Zhang, K., P. J. Rasch, M. A. Taylor, H. Wan, L.-Y. R. Leung, P.-L. Ma, J.-C. Golaz,
894 J. Wolfe, W. Lin, B. Singh, S. Burrows, J.-H. Yoon, H. Wang, Y. Qian, Q. Tang,
895 P. Caldwell, and S. Xie (2017), Impact of numerical choices on water conservation in
896 the e3sm atmosphere model version 1 (eam v1), *Geoscientific Model Development Dis-
cussions*, 2017, 1–26, doi:10.5194/gmd-2017-293.

```

do nt=1,ntotal

PARAMETERIZATIONS:
Last dynamics state received from dynamics
output 'pBF'
efix Energy fixer
output 'pBP'
phys param Physics updates the state and state saved for energy fixer
output 'pAP'
pwork Pressure work (dry mass correction)
output 'pAM'
Physics tendency (forcing) passed to dynamics

DYNAMICAL CORE
output 'dED'
do ns=1,nsplit
output 'dAF'

phys
START PHYSICS-DYNAMICS COUPLING
Update dynamics state with (1/nsplit) of physics tendency (ftype=2)
if (ns=1) Update dynamics state with entire physics tendency (ftype=1)
DONE PHYSICS-DYNAMICS COUPLING

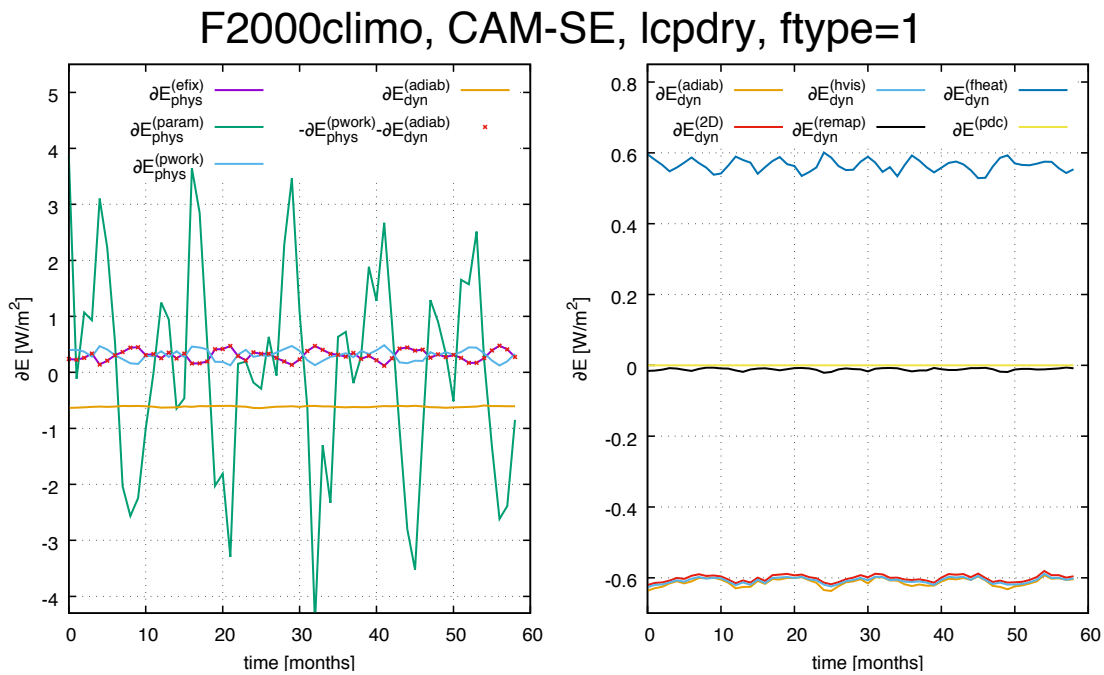
output 'dB'D'

adiab
2D
do nr=1,rsplit
Advance the adiabatic frictionless equations of motion
in floating Lagrangian layer
do ns=1,hypervis_subcycle
output 'dBH'
hvis
fheat Apply hyperviscosity operators
output 'dCH'
Add frictional heating to temperature
output 'dAH'
end do (ns=1,hypervis_subcycle)
end do (nr=1,rsplit)
output 'dAD'
remap
Vertical remapping from floating Lagrangian levels to Eulerian levels
output 'dAR'
end do (ns=1,nsplit)
Dynamics state saved for next model time step and passed to physics
output 'dB'F'

end do (nt=1,ntotal)

```

315 **Figure 1.** Pseudo-code for CAM-SE showing the order in which relevant physics updates are performed as
 316 well as dynamical core steps and associated loops. In green font locations where the state is captured and out-
 317 put is shown together with its 3 character identifier. The outer most loop (1, *ntotal*) advances the entire model
 318 Δt_{phys} seconds (in this case 1800s). The dynamical core loops are as follows: the outer loop is the vertical
 319 remapping loop (1, *nsplit*) with associated time-step $\Delta t_{phys}/nsplit$. For stability the temporal advance-
 320 ment of the equations of motion in the Lagrangian layer needs to be sub-cycled *rsplit* times. Within the
 321 *rsplit*-loop the hyperviscosity time-stepping is sub-cycled *hypervis_subcycle* times (again for stability).
 322 For more details on the time-stepping in CAM-SE see Lauritzen *et al.* [2018].



479 **Figure 2.** Monthly averaged TE tendencies as a function of time for various aspects of the TE consistent
 480 configuration of CAM-SE run in AMIP-type configuration with perpetual year 2000 SSTs. Left Figure shows
 481 $\partial \hat{E}$ TE tendencies in physics and, for comparison, TE tendency for the adiabatic dynamical core. The right
 482 plot shows the **breakdown** of $\partial \hat{E}$ for the dynamical core. These plots show that the energy tendency from the
 483 dynamical core is quite constant (to within $\sim 0.02 W/m^2$ or less) so only one month simulations is adequate to
 484 assess energy diagnostics for the dynamical core. For more details see Section 3.1.

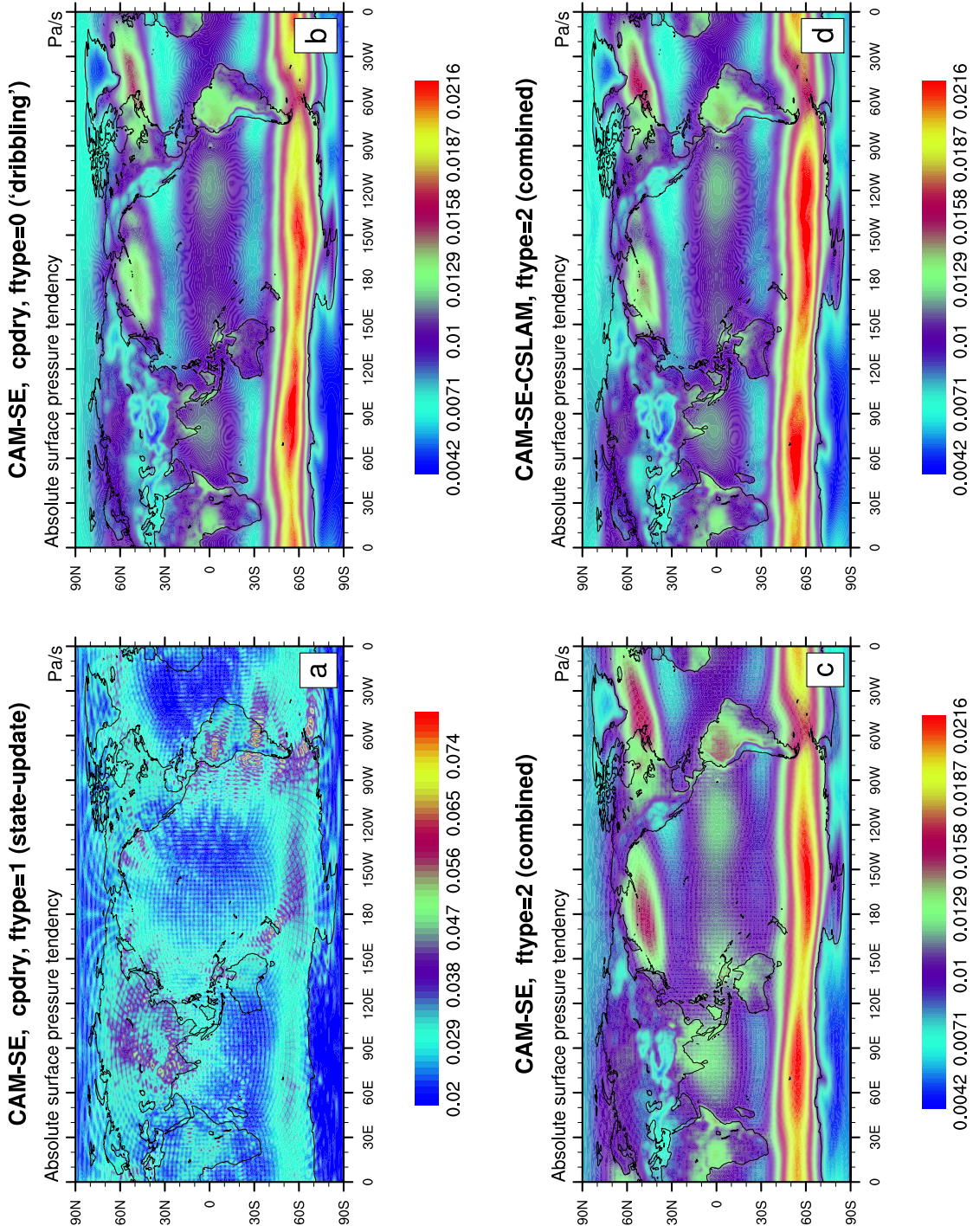


Figure 3. One year average of the absolute surface pressure tendency for (a) the TE consistent configuration, (b) ‘dribbling’ physics-dynamics coupling, (c) ftype=2 physics-dynamics coupling and (d) CSLAM version of CAM-SE, respectively. (a) has a closed physics-dynamics coupling budget but spurious noise, (b) has no spurious noise but the mass-budget in physics-dynamics coupling is not closed (see Figure 6), (c) has a closed mass budget in physics-dynamics coupling but some spurious noise at element boundaries which is eliminated when using CAM-SE-CSLAM (d). Note, the smallest value in panel (a) is the largest in panels (b), (c) and (d).

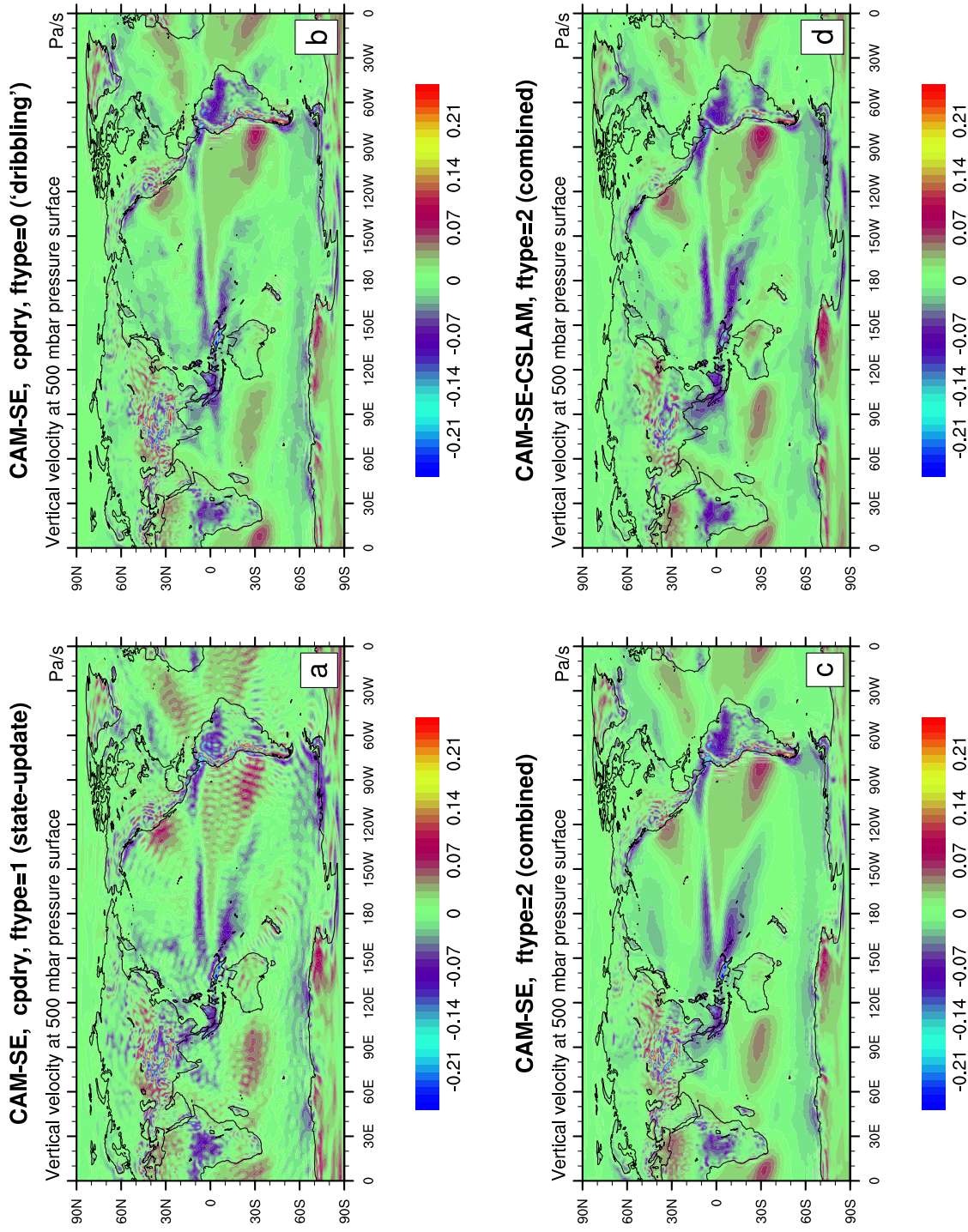


Figure 4. Same as Figure 3 but for 500hPa vertical pressure velocity. Note the ringing patterns off the West coast of South America and around the Himalayas in CAM-SE (a-c) that are eliminated with CAM-SE-CSLAM (d) that makes use of a quasi equal-area physics grid.

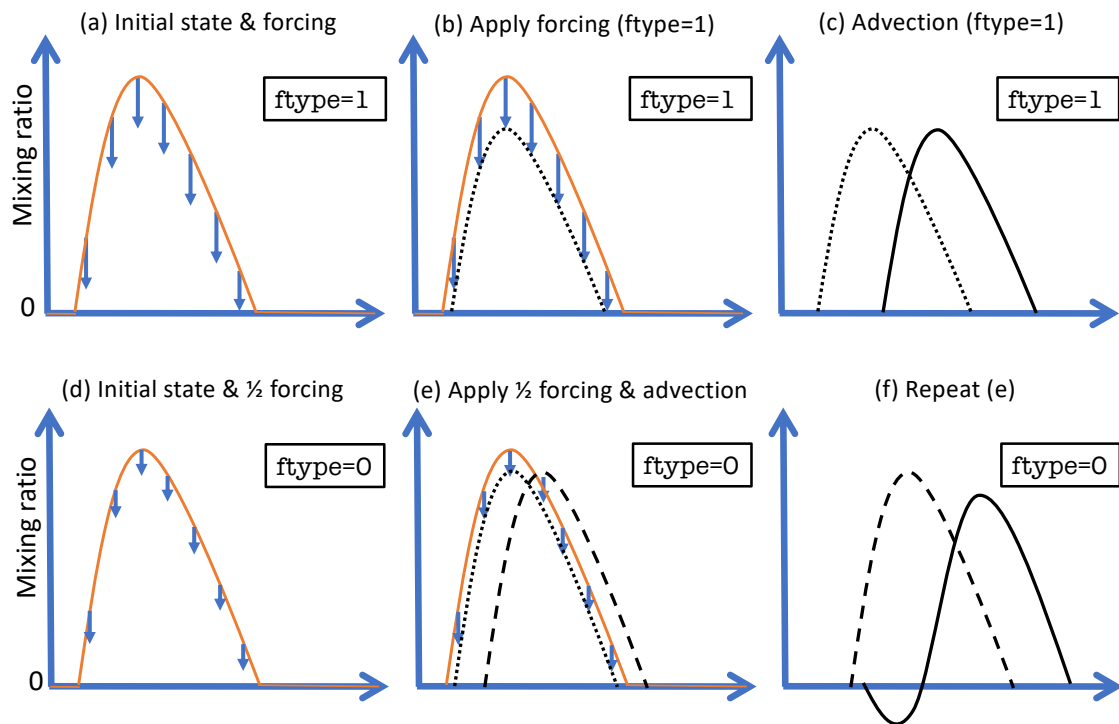


Figure 5. A schematic of state-update ($\text{ftype}=1$; row 1) and ‘dribbling’ ($\text{ftype}=0$; row 2) physics-dynamics coupling algorithms. See Section 3.2 for details.

F2000climo, CAM-SE, cpdry, ftype=0 ('dribbling')

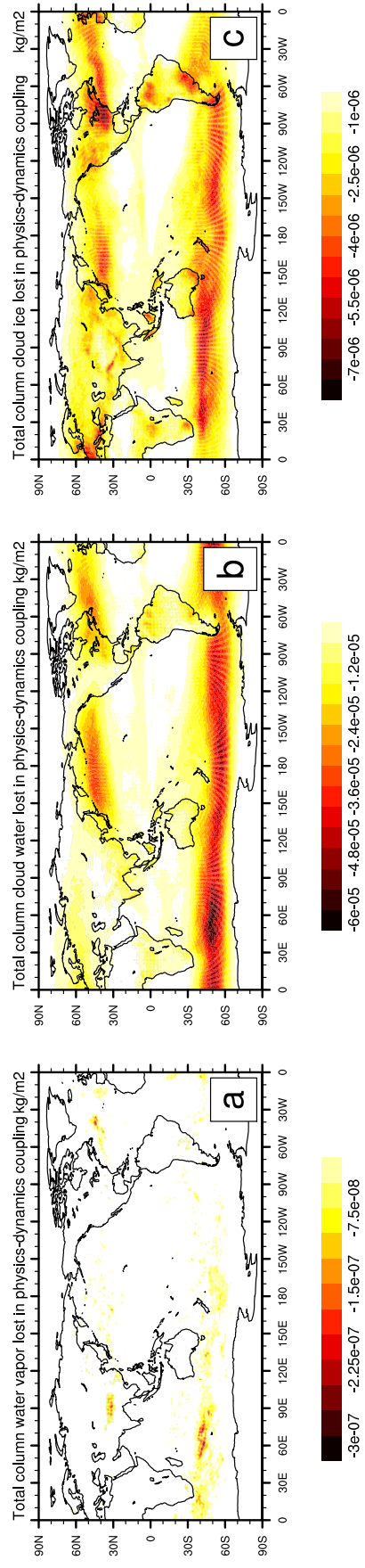
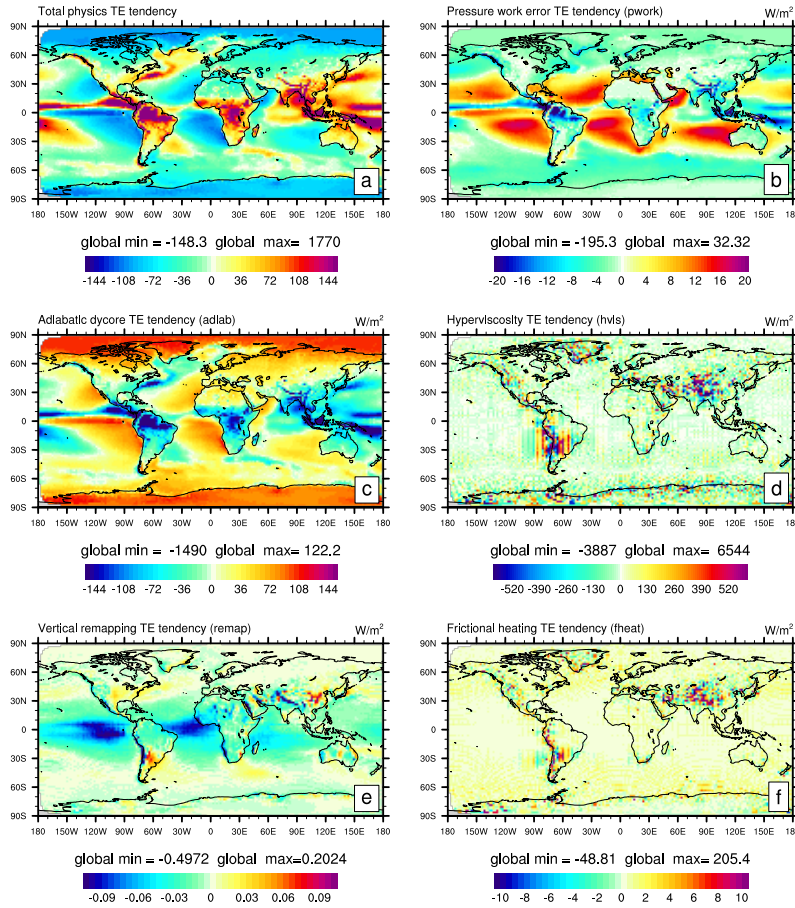


Figure 6. One year average of mass [kg/m^2] ‘clipped’ in physics-dynamics coupling (so that state is not driven negative) when using `ftype=0` (‘dribbling’) physics-dynamics coupling for (a) water vapor, (b) cloud liquid and (c) cloud ice, respectively. Interestingly the element boundaries systematically show in the plots which is likely related to the anisotropy of the quadrature grid [Herrington *et al.*, 2018].

TE tendencies for the default CAM-SE configuration (AMIP)



663 **Figure 7.** Two-dimensional spatial structure of column-integrated TE tendencies for different terms in
 664 the TE tendency budget using the *default* configuration: Column-integrated (a) $\partial E^{(\text{param})}$, $\partial E^{(p_{\text{work}})}$,
 665 $\partial E^{(\text{adiab})}$, $\partial E^{(\text{hvvis})}$, $\partial E^{(\text{remap})}$, and $\partial E^{(\text{fheat})}$. Above each color bar the global minimum and maximum
 666 TE tendencies are noted as there a small number of grid points where the TE tendencies are much larger than
 667 the color bar range.